Chemical Physics Letters 474 (2009) 18–22

Contents lists available at ScienceDirect

Chemical Physics Letters

journal homepage: www.elsevier.com/locate/cplett

Time-dependent wave packet calculation of the LiH + H reactive scattering on a new potential energy surface

Frederico V. Prudente [a,*], Jorge M.C. Marques [b], Angelo M. Maniero [c]

[a] Instituto de Física, Universidade Federal da Bahia, 40210-340 Salvador, BA, Brazil
[b] Departamento de Química, Universidade de Coimbra, 3004-535 Coimbra, Portugal
[c] Instituto de Ciências Ambientais e Desenvolvimento Sustentável, Universidade Federal da Bahia, 47805-100 Barreiras, BA, Brazil

ARTICLE INFO

Article history:
Received 4 March 2009
In final form 8 April 2009
Available online 11 April 2009

ABSTRACT

A new potential energy surface is proposed for the ground electronic state of LiH_2 and the quantum wave packet calculation for LiH + H reaction is performed. The full configuration interaction method and an aug-cc-pVQZ basis set are employed to calculate the potential energy for a set of criteriously selected geometries. The many-body expansion procedure is used to describe the analytical PES function. The new PES leads to a very different wave packet dynamics for both exothermic (Li + H_2) and thermoneutral (H + LiH) reactions when compared with the previous ones.

1. Introduction

The lithium chemistry has received a great attention in recent years due to the importance that LiH molecules and its ionic variants can have in the primordial universe [1–4]. In particular, it is believed that the formation and depletion of LiH and LiH^+ species play an important role in deviations of Cosmic Background Radiation spectrum [5]. Such processes have been studied in detail and possible depletion pathways, via collisions with H^+ and H, have been envisaged by Stancil et al. [6,7]. In this context, the highly exothermic reaction

$$LiH + H \rightarrow Li + H_2 \quad (1)$$

is considered to contribute to LiH depletion, while the thermoneutral hydrogen-exchange reaction

$$LiH_a + H_b \rightarrow H_a + LiH_b \quad (2)$$

leads to the retention of LiH in this process.

For the theoretical study of the reactions (1) and (2), it is necessary to calculate the relevant potential energy surface (PES) describing the interaction in the molecular system. The ground state potential energy surface of LiH_2 system was initially obtained for the collinear arrangement by Clarke et al. [8] through the application of the spin-coupled valence bond (SCVB) non-orthogonal configuration interaction (CI) method. Their results [8] establish that reaction (1) is strongly exothermic (by about 2.0238 eV) and presents an early small barrier of ~0.036 eV in the LiH + H entrance channel. In turn, Dunne, Murrell and Jemmer (DMJ) [9] have reported the first three-dimensional LiH_2 PES by fitting their Full CI *ab initio* points to an adequate analytical function within the many-body expansion (MBE) framework [10]; in contrast, the DMJ potential [9] does not show any barrier for the approaching reactants. More recently, Kim et al. [11] employed the interpolant moving least squares (IMLS)/Shepard scheme [12,13] to fit multireference CI (MRCI) electronic energies and concluded about the direct nature of reaction (1).

Although classical [8,9,11] and quantum [8] dynamics were performed in the aforementioned papers, only the analytical potential energy surface of Dunne et al. [9] has been employed in several theoretical studies by using time-dependent wave packet methodologies [14–19]. Specifically, $J = 0$ wave packet calculations on the title system have shown that the H-exchange reaction dominates over LiH depletion [14]. On the other side, the calculation of initial state-selected and channel specific energy-resolved LiH + H reaction probabilities using the DMJ potential surface [9] reveals signature of resonances in the corresponding probability curves of both reactions (1) and (2) at low energies [14]; resonances can last for a long time (~250 fs) at low energies and they become usually broad at high energies [15]. However, the DMJ LiH_2 PES [9] presents an unphysical well for non-collinear geometries in the Li—H_2 asymptotic valley (see the discussion in Section 2); this may be relevant for the dynamics of the title reaction. Specially, it is expected that resonances arising from the trapped wave packet in the well will rather complicate the dynamical behavior of the system. In particular, we have shown such a typical behavior for a simpler unidimensional system involving two diabatic electronic states [20].

The present Letter endehavours to contribute for a better knowledge of the title reaction. For that, we performed wave packet dynamics calculations of reactions (1) and (2) on a new LiH_2 PES, which clearly improves the corresponding ground

* Corresponding author. Fax: +55 71 32836606.
E-mail addresses: prudente@ufba.br (F.V. Prudente), qtmarque@ci.uc.pt (J.M.C. Marques), maniero@ufba.br (A.M. Maniero).

0009-2614/$ - see front matter © 2009 Elsevier B.V. All rights reserved.
doi:10.1016/j.cplett.2009.04.016

electronic potential of Dunne et al. [9]. This is achieved by performing accurate *ab initio* full configuration interaction (FCI) calculations and fitting them to a slightly modified analytical DMJ function (Section 2). Then, the dynamics were carried out by applying the real wave packet approach of Gray and Balint-Kurti [21], which is surveyed in Section 3.1. The resulting reaction probabilities are reported and discussed in Section 3.2. Finally, Section 4 summarizes the major achievements and gives a perspective of future work on this system.

2. Potential energy surface

The analytical functional form of the LiH_2 three-dimensional potential energy surface proposed here is based on the many body expansion formalism [10]:

$$V_{LiH_2}(R_1,R_2,R_3) = V^{(2)}_{LiH}(R_1) + V^{(2)}_{LiH}(R_2) + V^{(2)}_{HH}(R_3) + V^{(3)}(R_1,R_2,R_3), \tag{3}$$

where R_1, R_2 and R_3 are the Li—H_a, Li—H_b and H—H distances. The two-body terms ($V^{(2)}_{LiH}$ and $V^{(2)}_{HH}$) are represented by an extension [22] of the function proposed by Korona et al. [23],

$$V^{(2)}(R) = \begin{cases} \sum_{i=0}^{5} A_i R^{i-1} \exp(-\alpha R - \beta R^2) + \sum_{n=3}^{5} f_{2n}(bR)\frac{C_{2n}}{R^{2n}}, & R \geqslant R_0, \\ \frac{\tilde{A}\exp(-\tilde{\alpha}R)}{R}, & R < R_0, \end{cases} \tag{4}$$

where $A_i\,(i = 0,\ldots,5), \alpha, \beta$ and b are the fitting parameters, while C_{2n} are the dispersion coefficients (taken from Ref. [24]); $\tilde{A}$ and $\tilde{\alpha}$ have been calculated so that both potential and first derivatives of the two branches coincide at $R_0 = 0.15$ Å. Moreover, $f_{2n}(bR)$ are the Tang–Toennies damping functions [25] given by

$$f_{2n}(bR) = 1 - \exp(-bR)\sum_{k=0}^{2n}\frac{(bR)^k}{k!}. \tag{5}$$

Note that, following the same strategy as Patkowski et al. [22] for Ar_2, we have adopted a two-branch function for the diatomic potentials (Eq. (4)) to avoid problems in their practical application. Indeed, the first branch of Eq. (4) is adequate for the configuration space region of interest in the present work, but presents unphysical behavior for very short internuclear distances (typically $R < 0.1$ Å).

The three-body term ($V^{(3)}$) assumes the form:

$$V^{(3)}(R_1,R_2,R_3) = V_0\left[1 + \sum_{i,j,k} C_{ijk} S_1^i S_2^j S_3^k\right]\left[1 - \tanh\left(\gamma_1\frac{\rho_1}{2}\right)\right] \times \left[1 - \tanh\left(\gamma_1\frac{\rho_2}{2}\right)\right]\left[1 - \tanh\left(\gamma_3\frac{\rho_3}{2}\right)\right], \tag{6}$$

where $S_1 = R_1 + R_2 - 2R^e_{LiH}, S_2 = R_1 - R_2, S_3 = \rho_3 = R_3 - R^e_{HH}$ and $\rho_i = R_i - R^e_i,\ i = 1,2$. We point out that the present PES differ from the DMJ functional in the form of the diatomic potentials and the damping factor of the three body term (see Eq. (4) of Ref. [9]).

To model the PES, we have performed FCI calculations for the LiH_2, LiH, and H_2 species in their ground electronic states. All these calculations have been carried out with the GAMESS [26,27] package, using the augmented correlation consistent polarization valence quadruple zeta (aug-cc-pVQZ) basis set for H and Li atoms. The aug-cc-pVQZ set, proposed by Dunning Jr. [28], has been obtained from of the website *Basis Set Exchange (bse.pnl.gov/bse/portal)* [29,30]. This basis set comprises 215 Gaussian basis functions: a (7s,4p,3d,2f) → [5s,4p,3d,2f] contraction for hydrogen and a (13s,7p,4d,3f,2g) → [6s,5p,4d,3f,2g] contraction for lithium.

For LiH_2, the set of geometries used in the construction of the PES was carefully chosen using the following procedure: (i) the majority of the points were chosen by scanning the configuration space in a systematic way, so that they account for all of the PES (without any special care about the relevant topographic features of the potential); (ii) the remaining geometries were criteriously selected in regions of space that need to be well described in order to obtain an accurate PES for both the exothermic (Li + H_2) and the H-exchange reactions (*e.g.*, in the neighborhood of the minimum energy path and for geometries corresponding to the spurious minimum arising the DMJ PES).

Moreover, all the *ab initio* energies have been corrected for the basis set superposition error (BSSE) using the counterpoise (CP) method proposed by Boys and Bernardi [31]; a recent discussion of the CP correction for LiH molecule is presented in Ref. [32]. In particular, the correction for the three-body contribution of the *ab initio* electronic energies has been calculated as follows:

$$\Delta E^{(3)}_{LiH_2} = E^{LiH_2}_{LiH_2} - E^{LiH_2}_{LiH_a} - E^{LiH_2}_{LiH_b} - E^{LiH_2}_{H_2} + E^{LiH_2}_{Li} + E^{LiH_2}_{H_a} + E^{LiH_2}_{H_b}, \tag{7}$$

where $E^{LiH_2}_{LiH_2}$ is the total electronic energy of LiH_2, and $E^{LiH_2}_{LiH_a}, E^{LiH_2}_{Li\,H_b}$ and $E^{LiH_2}_{H_2}$ are the electronic energies of diatomics calculated using the complete LiH_2 atomic basis set, and $E^{LiH_2}_{Li}, E^{LiH_2}_{H_a}$ and $E^{LiH_2}_{H_b}$ are the atomic energies obtained using the same basis set.

The fit of the PES was done in two steps: first, the two-body terms (Eq. (4)) were fitted to the corresponding BSSE-corrected *ab initio* points; then, the remaining term of the many-body expansion (*i.e.*, Eq. (6)) was fitted to the three-body BSSE-corrected *ab initio* energies (*cf.*, Eq. (7)). The two- and three-body parameters of the analytical MBE potential function are shown in Tables 1 and 2, respectively. The fitted PES describes accurately the behavior of the *ab initio* points, showing the root-means square deviation (*rmsd*) of 0.064 eV. For example, the equilibrium geometry and the dissociation energy of both LiH ($R_e = 1.6075$ Å and $D_e = 20092\ cm^{-1}$) and H_2 ($R_e = 0.7416$ Å and $D_e = 38181\ cm^{-1}$) diatomic potentials are in excellent agreement with the experimental ones: $R_e = 1.5956$ Å and $D_e = 20288\ cm^{-1}$ for LiH [33]

Table 1
Fitted parameters for H_2 and LiH diatomic potentials. Energy is in eV and distance is in Å.

H_2 ($X^1\Sigma_g^+$)				LiH ($X^1\Sigma^+$)			
A_0	31.59401	A_1	−150.5357	A_0	115.5955	A_1	−336.4882
A_2	974.1085	A_3	−1269.879	A_2	532.1033	A_3	−440.1544
A_4	1139.014	A_5	−642.5568	A_4	177.1042	A_5	−33.62282
α	4.514618	β	0.055125	α	1.605378	β	0.208769
b	5.083533	$\tilde{A}$	28.40989	b	2.568512	$\tilde{A}$	117.1488
$\tilde{\alpha}$	7.66646			$\tilde{\alpha}$	4.58692		

Table 2
Fitted parameters for the three-body term (Eq. (6)) of the LiH_2 potential energy surface. Energy is in eV and distance is in Å.

C_{100}	0.573310	C_{001}	0.390592
C_{200}	0.163482	C_{020}	−0.050389
C_{002}	−1.157114	C_{101}	0.603342
C_{300}	0.029562	C_{003}	0.785840
C_{120}	0.171082	C_{021}	0.148571
C_{102}	−0.972644	C_{201}	0.184990
C_{400}	0.014036	C_{004}	−0.117217
C_{301}	0.058156	C_{220}	0.040418
C_{202}	−0.126546	C_{103}	0.334104
C_{121}	−0.197524	C_{040}	0.055862
C_{022}	−0.084976	γ_1	1.454945
γ_3	0.829355	V_0	5.953328
R^e_{HH}	0.7414	R^e_{LiH}	1.5953

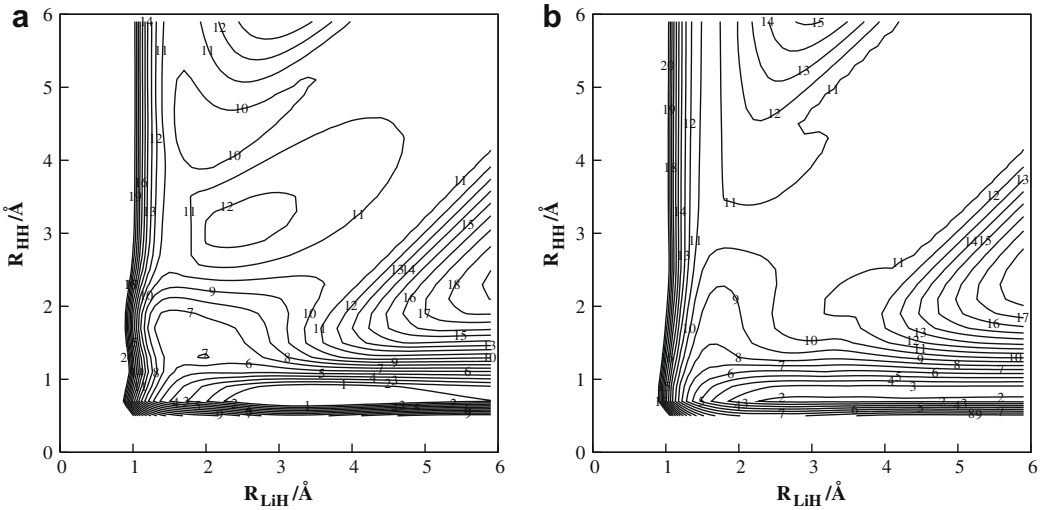

Fig. 1. Relaxed contour plot for the LiH_2 PES: (a) DMJ potential [9]; (b) new potential. The first contour is at −4.850 eV and the separation between consecutive contours is 0.241 eV.

and $R_e = 0.7414$ Å and $D_e = 38288$ cm^{-1} for H_2 [34]. Furthermore, our results are in better agreement with the experimental data than those of Kim et al. [11].

Fig. 1 shows isoenergetic contours diagrams as function of R_{H-H} and one of the R_{Li-H} distances, while the corresponding angle is relaxed between 0° and 180°, for both DMJ (panel (a)) and present (panel (b)) potential energy surfaces. It is clear from Fig. 1a that the DMJ potential presents unphysical wells in the Li—H_2 and H–LiH asymptotic valleys; for example, the unphysical minimum in the Li—H_2 valley has an energy of −0.869 eV, and arises at the geometry $R_{Li-H} = 3.424$ Å, $R_{Li-H} = 3.424$ Å and $R_{H-H} = 0.725$. It is worth noting that these undesirable wells are not present in the new LiH_2 PES, as it can be observed in Fig. 1b. It is also apparent from Fig. 1 that the new PES is smoother than the DMJ one.

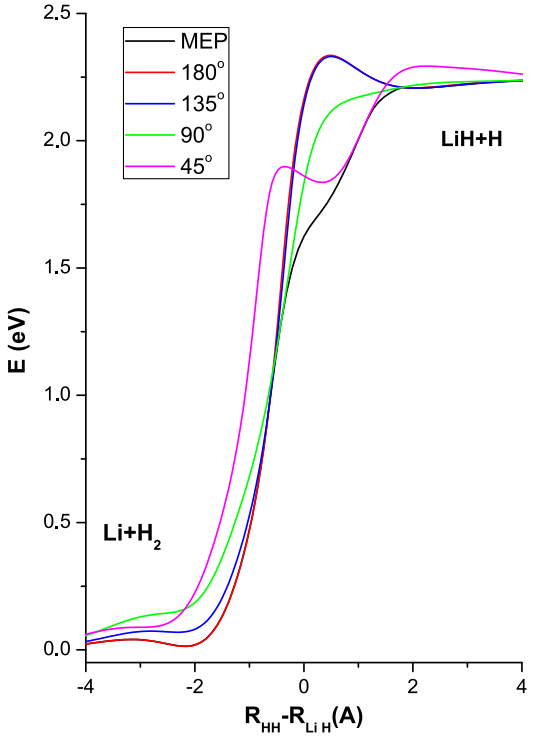

Fig. 2. Reaction profile along the absolute minimum energy path and for the ∠LiHH angle fixed at 180° (collinear), 135°, 90° and 45°.

The minimum energy paths (MEPs) as function of $R_{HH} - R_{LiH}$ coordinate of the new LiH_2 PES are shown in Fig. 2. Specifically, the figure shows the MEPs obtained for the ∠LiHH angle fixed at 180° (collinear geometry), 135°, 90° and 45°; also shown is the MEP obtained by relaxing the ∠LiHH angle. Note that the reaction is preferentially collinear at the Li + H_2 channel, but a similar behavior is not observed in the strong interaction region and at the H + LiH channel. Moreover, whilst a small barrier (*i.e.*, 0.036 eV) along the minimum energy path for reaction (1) has been identified by Clarke et al. [8] (and also shown in Fig. 2 for the curve corresponding to the collinear approach), no barrier is noticed in both DMJ and new potential surface.

3. Quantum dynamics calculations

3.1. Real wave packet method

The real wave packet (RWP) procedure developed by Gray and Balint-Kurti [21] is employed in this work to perform the quantum time-dependent dynamics calculations. This method has been widely used to study atom–diatom reaction with $J = 0$ (see Refs. [17,35–37], and references therein) and it was recently extended to $J \geqslant 0$ calculations in the DIFFREALWAVE parallel code [38]. The RWP method is based on the solution of the time-dependent Schrödinger equation mapped as

$$i\hbar \frac{\partial \psi(R,r,\gamma,t)}{\partial t} = f(\widehat{H})\psi(R,r,\gamma,t), \tag{8}$$

where R, r, and γ are the appropriate Jacobi coordinates and the Hamiltonian is replaced by

$$f(\widehat{H}) = -\frac{\hbar}{\tau}\cos^{-1}(\widehat{H}_s). \tag{9}$$

The $\widehat{H}_s = a_s\widehat{H} + b_s$ operator is a scaled Hamiltonian with a_s and b_s chosen in such way that the minimum and maximum $\widehat{H}_s$ eigenvalues lie in $(-1, 1)$ range. Within this choice, only the real part of the wave packet is propagated using the damped Chebyshev iteration procedure [21,39,40]. In this work, we have used the function

$$A(R,r) = A_R(R)A_r(r) \tag{10}$$

Table 3
Grid and initial condition details for the RWP calculations in the products Jacobi coordinates. Values are given in atomic units, unless otherwise specified.

	Reaction (1)	Reaction (2)
Initial translational energy	0.4 (eV)	0.4 (eV)
Center (R_0) and width (α) of the initial WP	10.0 and 5.2	10.0 and 5.2
R' range and number of grid points	0.5–31.0 and 310	0.5–21.0 and 210
r' range and number of grid points	0.5–21.0 and 260	0.5–17.0 and 180
Number of angular basis functions	64	64
Cutoff energy	0.44	0.44
Beginning of the absorption region R' and r'	18.0 and 13.0	18.0 and 13.0
Absorption parameter	2.0	2.0
Asymptotic analysis at R'	17.0	17.0

as damping factor in the Chebyshev procedure to absorb the wave packet near the edges of the grid; in Eq. (10), A_x ($x = R$ or r) is given by

$$A_x(x) = \exp[-c_x \exp(-2(x_{max} - x_{abs})/(x - x_{abs}))] \quad (11)$$

for $x > x_{abs}$ and $A_x(x) = 1$ otherwise.

For the reaction A + BC → AB + C, two sets of Jacobi coordinates can be defined: the reactant ones, that are specified by the distance from A to the center of mass of BC (R), the B-C internuclear distance (r), and the corresponding Jacobi angle (γ); and the product ones, that comprise the distance from C to the center of mass of AB (R'), the A–B internuclear distance (r'), and the corresponding Jacobi angle (γ'). In the present study, the initial wave packet is written in reactant Jacobi coordinates, *i.e.*,

$$\psi(R, r, \gamma, t = 0) = g(R)\chi_{vj}(r)\phi_j(\cos\gamma), \quad (12)$$

being $\chi_{vj}(r)$ and $\phi_j(\cos\gamma)$ the initial vibrational and rotational states of BC diatomic, and

$$g(R) = N \exp[-ik_0(R - R_0)] \exp[-\beta(R - R_0)^2] \frac{\sin(\alpha(R - R_0))}{R - R_0}. \quad (13)$$

This particular choice of the $g(R)$ factor gives a smooth and relatively flat function for the initial momentum distribution, which provides more accurate results in the energetic extremes than a single Gaussian function [35]. Since one wants to obtain reaction probabilities in terms of the products coordinate system, the initial wave packet is transformed to coordinates R', r', and γ' by applying the Chebyshev iteration procedure [39,40].

3.2. Reaction probabilities

In order to compare the present three-dimensional PES with the DMJ one [9], time-dependent quantum dynamical calculations were performed using the RWP method for the highly exothermic (1) and the thermoneutral hydrogen-exchange (2) reactions. All important parameters employed in both calculations, including grid sizes, absorption parameters and initial conditions are presented in Table 3. Moreover, the real wave packet was propagated for 100 000 iterations to guarantee the convergence of the results in all calculations. This is necessary due to the known existence of resonances with a long lifetime in the reactions on the DMJ potential [15], making the wave packet take a long time to pass through the region where the asymptotic analysis is performed.

The reaction probabilities for the exothermic ($LiH + H(v = j = 0) \rightarrow Li + H_2$) and isoenergetic H-exchange ($LiH_a + H_b(v = j = 0) \rightarrow H_a + LiH_b$) reactions with $J = 0$ are displayed in Fig. 3. These represent the reaction probabilities for the particular channel which is a result of the summation over all open vibrational (v') and rotational (j') levels of the corresponding product diatomic molecule. We point out that the results obtained using the DMJ PES are in accordance with the previous ones calculated with another method by Padmanaban and Mahapatra (see Fig. 6 of Ref. [14]).

The reaction probabilities depicted in Fig. 3 show significant different patterns when using the DMJ potential or the new PES. In particular, it is observed that the exothermic reaction is more efficient than the thermoneutral hydrogen-exchange reaction when the new LiH_2 PES is employed; the opposite trend is observed for the DMJ potential [9]. The results with the present PES indicate also a decrease of the total reaction probability (*i.e.*, the sum of exothermic and thermoneutral hydrogen-exchange probabilities), and the consequent increase of the nonreactive probability for high energies. This is the expected behavior for this type of reaction. Moreover, the reaction probabilities calculated with the new LiH_2 potential show resonance structures that are less evident than the ones obtained with the DMJ surface. Therefore, the previous studies of the title reaction [14–19], including the calculations of resonances, reaction cross section and thermal rate constant can be questionable in light of the present results, and hence should be revisited.

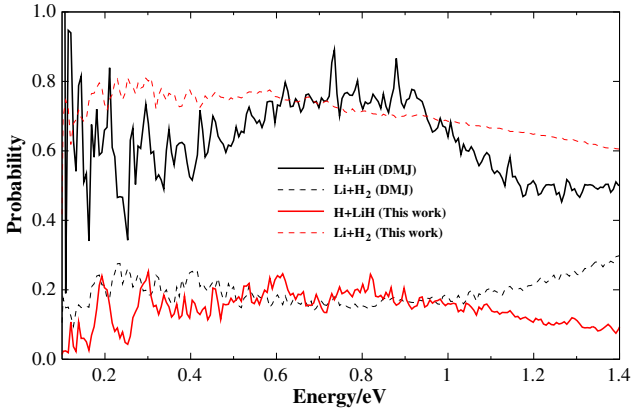

Fig. 3. Total reactive probabilities of the exothermic $LiH + H \rightarrow Li + H_2$ and thermoneutral hydrogen-exchange $LiH_a + H_b \rightarrow H_a + LiH_b$ reactions for the new and the DMJ [9] potential energy surfaces.

4. Concluding remarks

We have obtained an accurate potential energy surface for the ground electronic state of LiH_2 system which clearly improves the Dunne et al. potential [9] in several ways:

1. FCI/aug-cc-pVQZ *ab initio* calculations have been performed to model the present PES.
2. Although the simple analytical form used to represent the *ab initio* data is similar to the one applied in Ref. [9], the *rmsd* value obtained by us in the fitting procedure is lower than that reported for DMJ potential.

3. The present PES is quite smooth and does not present any unphysical well in the $Li + H_2$ and $H + LiH$ channels.

The $J = 0$ real wave packet calculations carried out on the new PES show a completely different pattern for the reaction probability of both $Li + H_2$ formation and H-exchange processes. It is worth noting that the reaction probability for the formation of $Li + H_2$ is higher than the corresponding value for the H-exchange channel in the whole range of energy studied, while the reverse pattern was found with the DMJ potential (*cf.* Ref. [14] and this work). This dynamical behavior obtained with the new PES is consentaneous with an exothermic barrierless reaction, which is expected for $LiH + H \rightarrow Li + H_2$. Whilst the reaction probabilities calculated with the DMJ potential for the title system are unlikely, our PES leads to the expected behavior for a competition between the isoenergetic H-exchange reaction and the exothermic formation of the $Li + H_2$ products.

The accurate analytical PES presented here can be used for further classical or quantum investigations concerning the dynamics and kinetics of all processes occurring in the ground electronic state of LiH_2 system. Indeed, the present work is the first step towards a more detailed analysis of the title system that will be reported in a forthcoming publication.

Finally, we point out that during the review process of the present Letter we were aware about the publication of another PES on the title system [41] which was obtained through interpolation of *ab initio* points calculated at multireference configuration interaction (MRCI) level of theory. Quantum dynamics calculations, such as those reported in this Letter for our potential, are needed to assess a quantitative comparison between the two PESs.

Acknowledgements

J.M.C.M. thanks Fundação para a Ciência e Tecnologia (FCT), Portugal, for the sabbatical Grant (SFRH/BSAB/636/2006). F.V.P. thanks Conselho Nacional de Desenvolvimento Científico e Tecnológico (CNPq), Brazil, for a grant. We are grateful to the John von Neumann Institut für Computing, Jülich, for the provision of supercomputer time on the IBM Regatta p690+ (Project EPG01).

References

[1] S. Lepp, J. Shull, Astrophys. J. 280 (1984) 465.
[2] A. Dalgarno, S. Leep, in: S.P. Tarafdar, M.P. Varshni (Eds.), Astrochemistry, Reidel, Boca Raton, 1987.
[3] S. Lepp, P.C. Stancil, A. Dalgarno, J. Phys. B: At. Mol. Opt. Phys. 35 (2002) R57.
[4] E. Bodo, F.A. Gianturco, R. Martinazzo, Phys. Rep. 384 (2003) 85.
[5] Y.K. Dubrovich, A.A. Lipovka, Astron. Astrophys. 296 (1995) 301.
[6] P.C. Stancil, S. Lepp, A. Dalgarno, Astrophys. J. 458 (1996) 401.
[7] P.C. Stancil, A. Dalgarno, Astrophys. J. 479 (1997) 543.
[8] N.J. Clarke, M. Sironi, M. Raimondi, S. Kumar, F.A. Gianturco, E. Buonomo, D.L. Cooper, Chem. Phys. 233 (1998) 9.
[9] L.J. Dunne, J.N. Murrell, P. Jemmer, Chem. Phys. Lett. 336 (2001) 1.
[10] J.N. Murrel, S. Carter, S.C. Farantos, P. Huxley, A.J.C. Varandas, Molecular Potential Energy Functions, Wiley, Chichester, 1984.
[11] K.H. Kim, Y.S. Lee, T. Ishida, G. Jeung, J. Chem. Phys. 119 (2003) 4689.
[12] T. Ishida, G.C. Schatz, J. Chem. Phys. 107 (1997) 3558.
[13] T. Ishida, G.C. Schatz, Chem. Phys. Lett. 298 (1998) 285.
[14] R. Padmanaban, S. Mahapatra, J. Chem. Phys. 117 (2002) 6469.
[15] R. Padmanaban, S. Mahapatra, J. Chem. Phys. 120 (2004) 1746.
[16] R. Padmanaban, S. Mahapatra, J. Chem. Phys. 121 (2004) 7681.
[17] P. Defazio, C. Petrongolo, P. Gamallo, M. González, J. Chem. Phys. 122 (2005) 214303.
[18] R. Padmanaban, S. Mahapatra, J. Phys. Chem. A 110 (2006) 6039.
[19] R. Padmanaban, S. Mahapatra, J. Theor. Comput. Chem. 5 (2006) 871.
[20] F.V. Prudente, A. Riganelli, J.M.C. Marques, Phys. Chem. Chem. Phys. 5 (2003) 2354.
[21] S.K. Gray, G.G. Balint-Kurti, J. Chem. Phys. 108 (1998) 950.
[22] K. Patkowski, G. Murdachaew, C.-M. Fou, K. Szalewicz, Mol. Phys. 103 (2005) 2031.
[23] T. Korona, H.L. Williams, R. Bukowski, B. Jeziorski, K. Szalewicz, J. Chem. Phys. 106 (1997) 5109.
[24] Z. Yan, J.F. Babb, A. Dalgarno, G.W.F. Drake, Phys. Rev. A 54 (1996) 2824.
[25] K.T. Tang, J.P. Toennies, J. Chem. Phys. 80 (1984) 3726.
[26] M.W. Schmidt et al., J. Comput. Chem. 14 (1993) 1347.
[27] M.S. Gordon, M.W. Schmidt, in: C.E. Dykstra, G. Frenking, K.S. Kim, G.E. Scuseria (Eds.), Theory and Applications of Computational Chemistry: The First Forty Years, Elsevier, Amsterdam, 2005, p. 1167.
[28] T.H. Dunning Jr., J. Chem. Phys. 90 (1989) 1007.
[29] D. Feller, J. Comput. Chem. 17 (1996) 1571.
[30] K.L. Schuchardt et al., J. Chem. Inf. Model. 47 (2007) 1045.
[31] F. Boys, F. Bernardi, Mol. Phys. 19 (1970) 553.
[32] M.S. Arruda, A.M. Maniero, F.V. Prudente, Rev. Mex. Fis., in press.
[33] W.C. Stwalley, W.T. Zemke, J. Phys. Chem. Ref. Data 22 (1993) 87.
[34] K.P. Huber, G. Herzberg, Molecular Spectra and Molecular Structure. IV Constants of Diatomic Molecules, Van Nostrand, New York, 1979.
[35] M. Hankel, G.G. Balint-Kurti, S.K. Gray, J. Chem. Phys. 113 (2000) 9658.
[36] W. Wang, C. Rosa, J. Brandão, Chem. Phys. Lett. 418 (2006) 250.
[37] M. Hankel, S.C. Smith, A.J.H.M. Meijer, J. Chem. Phys. 127 (2007) 064316.
[38] M. Hankel, S.C. Smith, R.J. Allan, S.K. Gray, G.G. Balint-Kurti, J. Chem. Phys. 125 (2006) 164303.
[39] V.A. Mandelshtam, H.S. Taylor, J. Chem. Phys. 102 (1995) 7390.
[40] V.A. Mandelshtam, H.S. Taylor, J. Chem. Phys. 103 (1995) 2903.
[41] M. Wernli, D. Caruso, E. Bodo, F.A. Gianturco, J. Phys. Chem. A 113 (2009) 1121.